

Submitted: August 1, 2024

Revised: September 5, 2024

Accepted: September 30, 2024

# The effect of the magnetron discharge power on the deposition rate of chrome coating obtained by sputtering an uncooled extended target

G.V. Kachalin , K.S. Medvedev , A.B. Tkhabisimov  , D.I. Iliukhin 

National Research University "Moscow Power Engineering Institute", Moscow, Russia

 abt-bkt@mail.ru

## ABSTRACT

The effect of the magnetron discharge power in the range from 2.2 to 8.2 kW on the deposition rate of chrome coatings obtained by spraying an uncooled and cooled planar extended target is studied. The coatings were applied to 12Cr18Ni10Ti stainless steel samples with temperature control using a chromel-copel thermocouple. It is shown that the deposition rate of coatings for an uncooled chrome target increases non-linearly with an increase in power of more than 6.5 kW, and at a power of 8.2 kW reaches 45  $\mu\text{m/h}$ , which is more than 2 times higher than for a cooled target. The results obtained indicate the prospects of using such extended magnetron systems to solve a number of applied problems in the energy sector, in particular, the formation of thermal barrier coatings on the domestic gas turbine blades.

## KEYWORDS

magnetron sputtering • cooled target • uncooled target • deposition rate • chrome coating • discharge power

**Acknowledgements.** The research was supported by the Ministry of Science and Higher Education of the Russian Federation within the framework of the state assignment "Development of physical and chemical foundations for the formation and prediction of properties of promising materials and coatings for energy conversion and storage systems" (FSWF-2023-0016).

**Citation:** Kachalin GV, Medvedev KS, Tkhabisimov AB, Iliukhin DI. The effect of the magnetron discharge power on the deposition rate of chrome coating obtained by sputtering an uncooled extended target. *Materials Physics and Mechanics*. 2025;53(2): 149–156.

[http://dx.doi.org/10.18149/MPM.5322025\\_13](http://dx.doi.org/10.18149/MPM.5322025_13)

## Introduction

Coatings of chromium and its compounds are widely used in industry. A chromium layer can be applied to provide corrosion protection or to increase surface hardness and wear resistance. The widely used galvanic chromium plating (electroplating) processes now face several restrictions due to the recognition of hexavalent chromium as a carcinogen in the 1990s. As a result, many countries have actively begun to develop and implement alternative chromium plating processes, among which physical vapor deposition (PVD) methods were the most widespread. However, all PVD processes developed to date still fall short of electroplating in three key criteria: productivity, cost and the ability to process large and elongated products. While recent years have seen the emergence of technological setups capable of handling products of varying dimensions [1,2], the challenge of improving PVD process efficiency remains unresolved.

One of the most widely used PVD processes is magnetron sputtering of a target by inert gas ions at reduced pressure. The devices implementing this process are called magnetron sputtering systems (MSS) [3–5].



Today, MSS are employed for depositing thin films and protective coatings in many industries due to their undeniable advantages: drop-free atomic flow, compatibility with any conductive materials and semiconductors and relative ease of scaling for large and elongated products [6–8]. The drawbacks of MSS include low deposition rates, target material utilization coefficient not exceeding  $30 \div 40 \%$  and a low percentage of ionization of sputtered atoms. The vast majority of industrial MSS use cooled ("cold") targets, where cooling is primarily necessary to prevent overheating of the magnetic system [9,10] rather than the processed products. In magnetron sputtering processes for coating formation in engineering applications, such as depositing erosion-resistant coatings on steam turbine blades or heat-resistant coatings on gas turbine blades, the temperature of the products can reach  $400\text{ }^{\circ}\text{C}$  or higher. For such tasks, cooled targets are not strictly necessary. Target heating occurs mainly due to the kinetic energy transferred to the target by accelerated ions generated in the magnetron discharge plasma burning region, leading to sublimation of material from the target surface. Sublimation significantly increases the deposition rate. The target material must have sufficient sublimation rates at its heating temperature, which is determined by the Hertz-Knudsen equation [11] (e.g., chromium or titanium). The target mounting design should minimize heat transfer to the magnetron's cooled parts, for example, by using thermal insulation gaskets. This positively affects the growing film's structure and enhances the productivity and cost-efficiency of the coating process.

Recently, several studies [12–28] have been published on uncooled chromium target sputtering, but these are research-oriented, as they used small planar round targets. In contrast, engineering applications require elongated planar targets comparable in size to the products. Elongated target sputtering (circa over 500 mm) presents technical challenges, particularly in ensuring uniform heating along the target's length, since the sublimation rate is a power function of temperature.

This study investigates the effect of discharge power on the deposition rate of chromium coatings formed by magnetron sputtering of an elongated uncooled target for industrial protective coating applications.

## Materials and Methods

The coatings were formed using a vacuum system developed at National Research University "Moscow Power Engineering Institute" [29,30], equipped with four elongated magnetrons arranged in opposing pairs ("face-to-face") at a distance of 300 mm. The magnetic fields of the magnetrons were synchronized to form a closed magnetic field in the space between them.

Thanks to the specialized planetary mechanism of the system's carousel, various processing and coating deposition modes could be implemented. In particular, it was possible to perform ion cleaning (etching) of samples using one pair of magnetrons while depositing coatings with the other pair, which was utilized in the present study.

Coating deposition was performed using a planar elongated magnetron with both cooled and uncooled targets made of chromium (99.9 %). The target dimensions were  $710 \times 65 \times 6\text{ mm}^3$ , with the uncooled target assembled from separate plates. A key feature

of the uncooled target's cathode assembly was its attachment to the magnetron through a thermal insulation gasket, ensuring low heat transfer and consequent target heating.

Coatings were deposited on polished 12Cr18Ni10Ti stainless steel samples measuring  $30 \times 40 \times 1 \text{ mm}^3$ . During the technological process, samples were mounted on a rotating fixture positioned in front of the magnetron. The target-to-fixture rotation axis distance was 150 mm. Experiments were conducted in high-purity argon atmosphere, with argon supplied to the vacuum chamber using an RRG-10 gas flow controller.

Target temperature was measured during the experiment using a chromel-alumel thermocouple with its tip installed at the target's side edge, allowing placement near the magnetron discharge zone. Sample temperature was monitored with a chromel-copel thermocouple with sample potential.

The coating process involved chamber preheating and high-vacuum pumping to  $5 \times 10^{-3} \text{ Pa}$  using a diffusion pump. Argon was supplied to the chamber with 15.3 NL/h (normal liters per hour) consumption during all experiments. Ion cleaning of sample surfaces was carried out in glow discharge with magnetron discharge support on cooled targets for 10 min across all power ranges. During cleaning the heating of uncooled targets was carried out. Temperature measurements showed the uncooled target reached steady-state conditions within 10 min across the entire applied power range from 2.2 to 10 kW. The sample fixture was then moved to the uncooled target's deposition zone and after that the coating was deposited. During coating, samples rotated directly in front of the target. For cooled target experiments, samples remained stationary and after cleaning the coating was deposited. Coating deposition time was 20 min for all experiments with -100 V bias voltage applied to samples. During transfer between cleaning and deposition zones for uncooled targets, samples temporarily assumed floating potential. Coating thickness was measured with Calotest Compact measuring device using ball cratering in accordance with ISO 1071-2, with deposition rates calculated from thickness data. For some experiments, metallographic microsections were manufactured, which were examined using a TESCAN MIRA 3 LMU scanning electron microscope.

## Results and Discussion

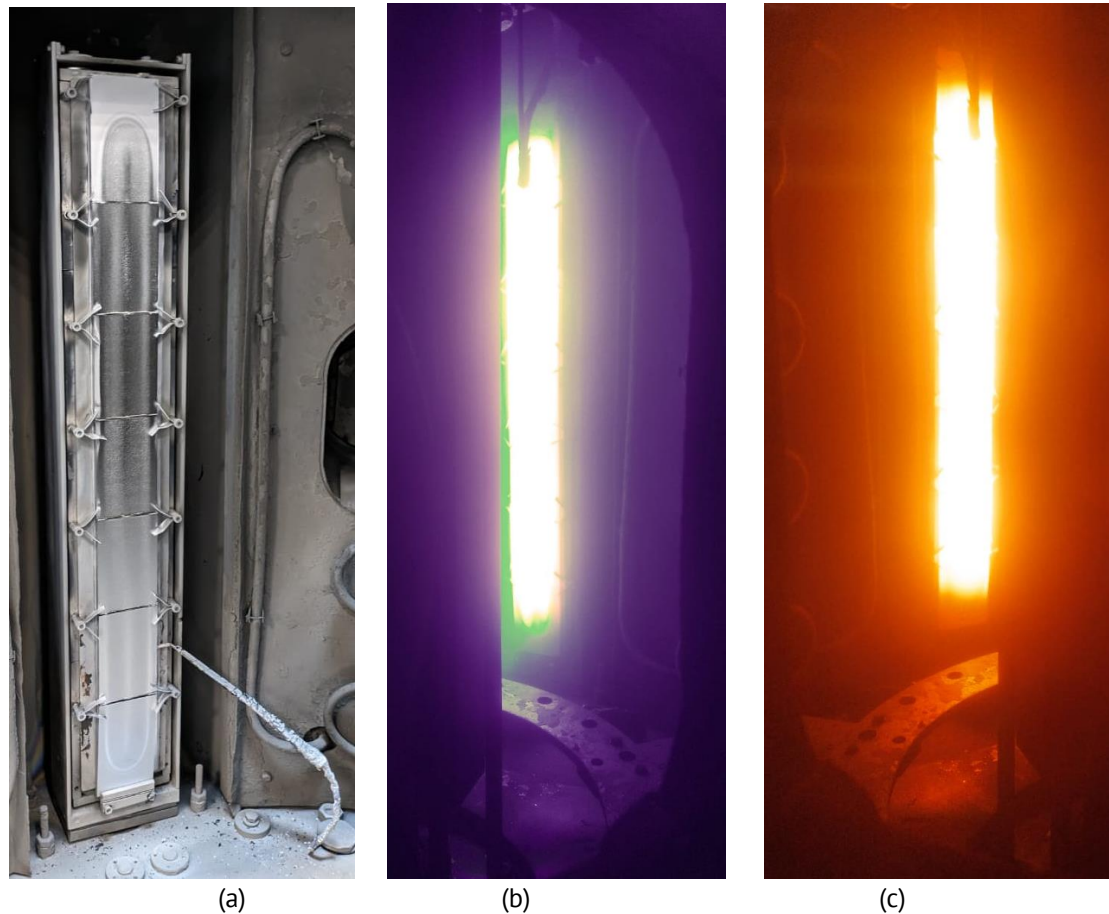
Figure 1 shows photographs of (a) an uncooled chromium target with an installed thermocouple in its lower part, (b) magnetron discharge on the surface of the uncooled target in argon plasma, (c) glow of the uncooled target immediately after turning off the magnetron discharge. Figure 1(b,c) demonstrates that target heating is uniform along its entire length. Table 1 presents the measured coating thickness and growth rate, as well as target and sample temperatures for the uncooled target.

Figure 2 shows the dependence of target temperature (curve 1) and sample temperature (curve 2) on discharge power in the range from 2.2 to 8.2 kW. Target temperature measurements were taken during brief turning offs of the discharge to avoid electromagnetic interference with the thermocouple.

Target temperature is a critical technological parameter that allows monitoring the onset of target material sublimation. The obtained dependencies of power influence on temperature (Fig. 2) and deposition rate (Fig. 3) are necessary for correlating target

temperature values with the beginning of its sublimation process, characterized by nonlinear growth in deposition rate.

Sample temperature is determined by the balance of power fluxes reaching its surface – the flow of sputtered atoms, crystallization heat, radiation from the heated target surface – and radiation from the sample surface [30]. The dependence of sample temperature on magnetron discharge power allows selecting a coating deposition mode that prevents changes in the sample's (product's) microstructure. Figure 3 shows the dependencies of chromium coating deposition rates obtained from the data in Table 1.



**Fig. 1.** Uncooled chromium target: (a) the thermocouple place of installation; (b) magnetron discharge in argon plasma; (c) the view immediately after turning off the discharge

**Table 1.** Coating thickness and growth rate and target and sample temperatures

| Power, kW | Cooled target                    |  | Uncooled target                  |  |  |  |
|-----------|----------------------------------|--|----------------------------------|--|--|--|
|           | Coating thickness, $\mu\text{m}$ | Coating growth rate, $\mu\text{m}/\text{hour}$ | Coating thickness, $\mu\text{m}$ | Coating growth rate, $\mu\text{m}/\text{hour}$ | Target temperature, $^{\circ}\text{C}$ | Sample temperature, $^{\circ}\text{C}$ |
| 2.2       | 1.74                             | 5.22   | 1.76                             | 5.3  | 679                                    | 335                                    |
| 3.2       | 2.6                              | 7.8  | 3.2                              | 9.6  | 876                                    | 374                                    |
| 4.1       | 3.2                              | 9.6  | 4.3                              | 12.9   | 993                                    | 400                                    |
| 5         | 4.0                              | 12.0   | 5.0                              | 15.0   | 1060                                   | 431                                    |
| 5.9       | 4.6                              | 13.8   | 6.0                              | 18.0   | 1114                                   | 446                                    |
| 6.5       | 5.0                              | 15.0   | 6.6                              | 19.8   | 1123                                   | 480                                    |
| 7.3       | 5.8                              | 17.4   | 8.2                              | 24.6   | 1158                                   | 498                                    |
| 8.2       | 6.5                              | 19.5   | 15.0                             | 45.0   | 1176                                   | 543                                    |

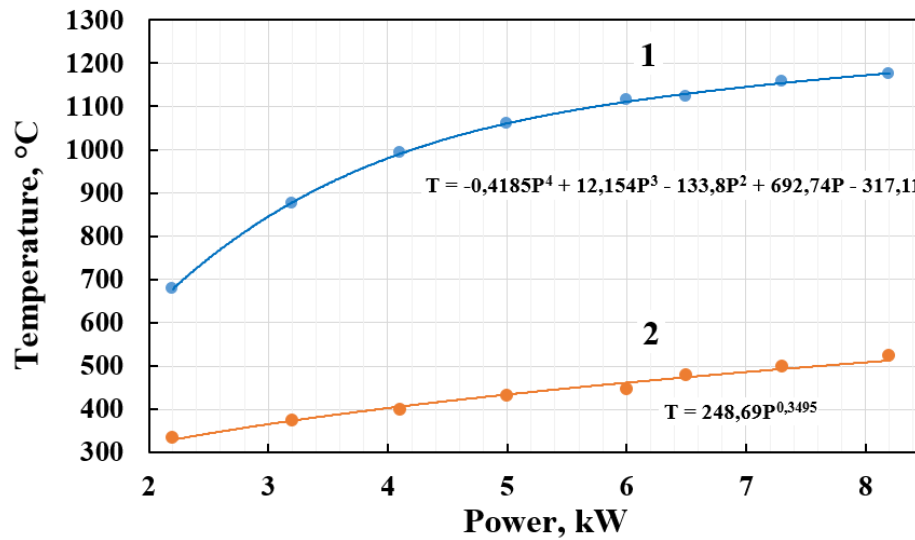


Fig. 2. Dependences of the temperature of the uncooled target (1) and sample (2) on the magnetron discharge power

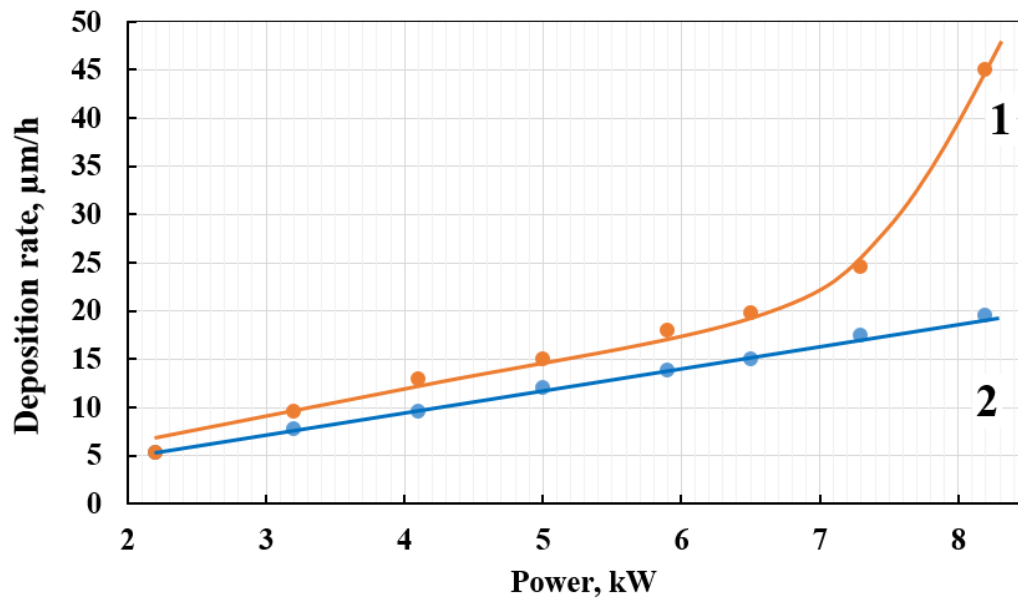


Fig. 3. Dependences of chromium coating growth rates on the magnetron discharge power for uncooled (1) and cooled (2) targets

Figure 3 demonstrates that at powers exceeding 6.5 kW, a nonlinear increase in coating growth rate is observed, caused by the addition of atoms evaporated from the target surface to the flow of sputtered atoms. At 8.2 kW power, the growth rate more than doubles, indicating equal flows of sputtered and evaporated chromium atoms from the target surface. Similar results were obtained for a magnetron with a small round uncooled target [17,31].

The obtained results demonstrate that increasing target temperature can significantly enhance chromium coating growth rates, which has substantial economic importance for industrial applications. Moreover, the sublimation process of target atoms



generally occurs from the entire heated target surface, which can improve target utilization efficiency.

Figure 4 shows that coatings in both cases (sputtering from cooled and uncooled targets) have dense columnar structures without visible pores or defects. However, in the case of the uncooled target (Fig. 4(b)), the chromium coating structure is finer-grained, with column widths ranging from 0.2 to 1.2  $\mu\text{m}$ , while sputtering from a cooled target (Fig. 4(a)) produces columns up to 3  $\mu\text{m}$  wide.

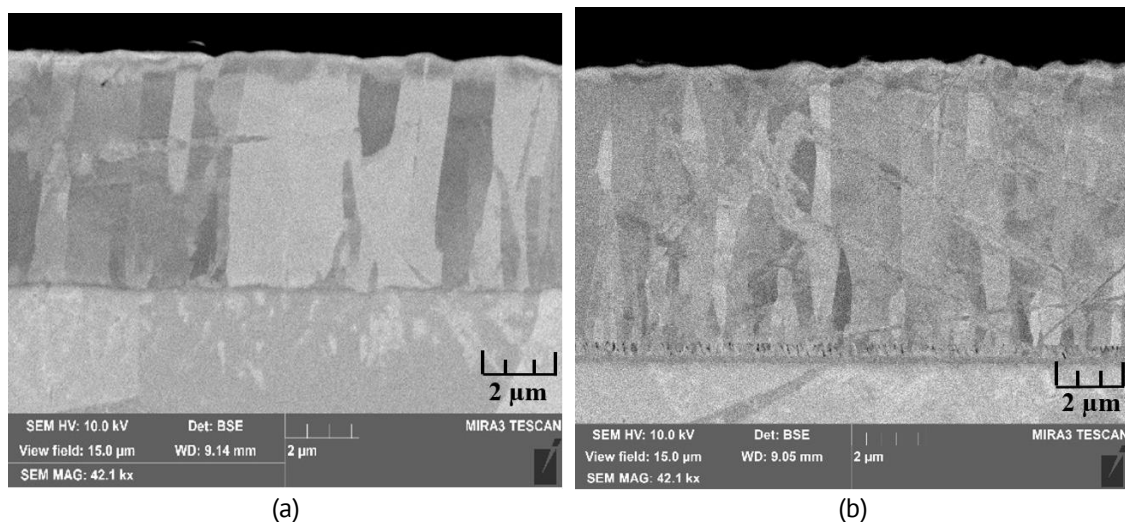


**Fig. 4.** Transverse sections of chromium coatings obtained by sputtering from a cooled (a) and uncooled (b) targets at a power range of 7.3 kW

Although the differences in coating structure may be insignificant in this particular case, they will inevitably affect coating properties. Furthermore, it should be expected that increasing coating growth rate through sublimation may reduce mechanical properties while increasing porosity and structural defects, due to the significant difference in energy between sputtered and evaporated atoms.

In [32], we investigated characteristics of chromium coatings obtained from an elongated uncooled target, which showed high adhesion and low roughness at high growth rates. However, we believe that optimal coating formation parameters will need to be determined for each specific application.







## Conclusions

As a result of a series of experiments on chromium coating formation using elongated cooled and uncooled targets, it was established that when increasing the magnetron discharge power above 6.5 kW (which in our experimental conditions corresponds to an uncooled target temperature exceeding 1100  $^{\circ}\text{C}$ ), a significant nonlinear increase in coating growth rate is observed.

At a magnetron discharge power of 8.2 kW, the growth rate of chromium coatings from an uncooled target more than doubles compared to the growth rate from a cooled target. This growth rate enhancement is associated with material sublimation from the target surface.

The results of this study were obtained for the first time and demonstrate the promising potential of using magnetrons with uncooled elongated targets to improve the efficiency and competitiveness of modern magnetron sputtering systems for industrial-scale protective coating formation.

## CRediT authorship contribution statement

**Gennadiy V. Kachalin**  : conceptualization, writing – original draft; **Konstantin S. Medvedev** : conceptualization, supervision; **Alexander B. Tkhabisimov**  : writing – review & editing, data curation; **Dmitriy I. Iliukhin** : investigation, data curation.

## Conflict of interest

The authors declare that they have no conflict of interest.

## References

1. Kachalin GV, Ryzhenkov AV, Medvedev KS, Bychkov AI, Parfenenok MA. Modern technological solutions for the formation of ion-plasma coatings on elements of fuel and energy complex equipment. *Safety and Reliability of Power Industry*. 2014;2: 8–12. (In Russian)
2. Li Y, Chen Y, Xu Z, Xia H, Natuski T, Xi Y, Ni Q. Effect of surface modification of carbon fiber based on magnetron sputtering technology on tensile properties. *Carbon*. 2023;204: 377–386.
3. Karlsson S, Eklund P, Österlund L, Birch J, Ali S. Effects of deposition temperature on the mechanical and structural properties of amorphous Al–Si–O thin films prepared by radio frequency magnetron sputtering. *Thin Solid Films*. 2023;787: 140135.
4. Yang Y, Zhang Y, Yan M. A review on the preparation of thin-film YSZ electrolyte of SOFCs by magnetron sputtering technology. *Separation and Purification Technology*. 2022;298: 121627.
5. Strzelecki GW, Nowakowska-Langier K, Mulewska K, Zieliński M, Kosińska A, Okrasa S, Wilczopolska M, Chodun R, Wicher B, Mirowski R, Zdunek K. Multi-component low and high entropy metallic coatings synthesized by pulsed magnetron sputtering. *Surface and Coatings Technology*. 2022;446: 128802.
6. Gudmundsson JT. Physics and technology of magnetron sputtering discharges. *Plasma Sources Science and Technology*. 2020;29: 113001.
7. Chodun R., Dypa M., Wicher B., Nowakowska-Langier K., Okrasa S., Minikayev R., Zdunek K. The sputtering of titanium magnetron target with increased temperature in reactive atmosphere by gas injection magnetron sputtering technique. *Applied Surface Science*. 2022;574: 151597.
8. Varavka VN, Kudryakov OV, Ryzhenkov AV, Kachalin GV, Zilova OS. Application of nanocomposite coatings to protect power equipment from droplet impact erosion. *Teplotenergetika*. 2014;11: 29–35. (In Russian).
9. Graillot-Vuillecot R, Thomann A-L, Lecas T, Cachoncinlle C, Millon E, Caillard A. Hot target magnetron sputtering process: Effect of infrared radiation on the deposition of titanium and titanium oxide thin films. *Vacuum*. 2020;181: 109734.
10. Hovsepian PE, Ehasarian AP. Six strategies to produce application tailored nanoscale multilayer structured PVD coatings by conventional and High Power Impulse Magnetron Sputtering (HIPIMS). *Thin Solid Films*. 2019;688: 137409.
11. Kupershtokh AL, Alyanov AV. Evaporation and condensation of pure vapor at the liquid surface in the method of lattice Boltzmann equations. *Numerical Methods and Programming*. 2022;23(4): 311–327. (In Russian).
12. Wang D, Zhong R, Zhang Y, Chen P, Lan Y, Yu J, Su GH, Qiu S, Tian W. Isothermal experiments on steam oxidation of magnetron-sputtered chromium-coated zirconium alloy cladding at 1200°C. *Corrosion Science*. 2022;206: 110544.
13. Kashkarov EB, Sidelev DV, Rombaeva M, Syrtanov MS, Bleykher GA. Chromium coatings deposited by cooled and hot target magnetron sputtering for accident tolerant nuclear fuel claddings. *Surface and Coatings Technology*. 2020;389: 125618.

14. Grudin VA, Bleykher GA, Sidelev DV, Yuriev YuN, Lomygin AD. Magnetron deposition of chromium nitride coatings using a hot chromium target: Influence of magnetron power on the deposition rate and elemental composition. *Surface and Coatings Technology*. 2022;433: 128120.
15. Shapovalov VI, Ahmedov H, Kozin AA, Demir A, Korutlu B. Simulation of the effect of argon pressure on thermal processes in the sputtering unit of a magnetron with a hot target. *Vacuum*. 2021;192: 110421.
16. Graillot-Vuillecot R, Thomann A-L, Lecas T, Cachoncinlle C, Millon E, Caillard A. Properties of Ti-oxide thin films grown in reactive magnetron sputtering with self-heating target. *Vacuum*. 2022;197: 110813.
17. Kaziev AV, Kolodko DV, Tumarkin AV, Kharkov MM, Lisenkov VYu, Sergeev NS. Comparison of thermal properties of a hot target magnetron operated in DC and long HIPIMS modes. *Surface and Coatings Technology*. 2021;409: 126889.
18. Bleykher GA, Borduleva AO, Krivobokov VP, Sidelev DV. Evaporation factor in productivity increase of hot target magnetron sputtering systems. *Vacuum*. 2016;132: 62–69.
19. Bleykher GA, Sidelev DV, Grudin VA, Krivobokov VP, Bestetti M. Surface erosion of hot Cr target and deposition rates of Cr coatings in high power pulsed magnetron sputtering. *Surface and Coatings Technology*. 2018;354: 161–168.
20. Sidelev DV, Bleykher GA, Bestetti M, Krivobokov VP, Vincenzo A, Franz S, Brunella MF. A comparative study on the properties of chromium coatings deposited by magnetron sputtering with hot and cooled target. *Vacuum*. 2017;143: 479–485.
21. Tang K, Li X, Wang C, Shen Y, Xu Y, Wen M. The application of NiCrPt alloy targets for magnetron sputter deposition: Characterization of targets and deposited thin films. *Thin Solid Films*. 2024;805: 140501.
22. Haneef M, Evaristo M, Morina A, Yang L, Trindade B. New nanoscale multilayer magnetron sputtered Ti-DLC/DLC coatings with improved mechanical properties. *Surface and Coatings Technology*. 2024;480: 130595.
23. Lee Y-C, Yen VC, Pithan C, Jan J-H. Study of Ni–Cr / CrN bilayer thin films resistor prepared by magnetron sputtering. *Vacuum*. 2023;213: 112085.
24. Grudin VA, Sidelev DV, Bleykher GA, Yuriev YuN, Krivobokov VP, Berlin EV, Grigoriev VYu, Obrosova A, Weiß S. Hot target magnetron sputtering enhanced by RF-ICP source for CrN<sub>x</sub> coatings deposition. *Vacuum*. 2021;191: 110400.
25. Xu Y, Li Y, Meng F, Huang F. Microstructure and multifunctionality of a 10-μm-thick dense yet smooth Cr(C) coating prepared by low-temperature magnetron sputtering. *Surface and Coatings Technology*. 2022;435: 128255.
26. Larhlimi H, Ghailane A, Makha M, Alami J. Magnetron sputtered titanium carbide-based coatings: A review of science and technology. *Vacuum*. 2022;197: 110853.
27. Sun Q, Wang J, Xie Y, Hu Y, Jiang Q, Zhang F, Wu T, Si Y, Qiao Z, Yigit K, Li Z, Li H, Wang S. Preparation and properties of chromium protective coatings on lithium targets for accelerator-based neutron sources. *Vacuum*. 2024;224: 113151.
28. Lin J, Stinnett TC. Development of thermal barrier coatings using reactive pulsed dc magnetron sputtering for thermal protection of titanium alloys. *Surface and Coatings Technology*. 2020;403: 126377.
29. Ryzhenkov VA, Sidorov SV, Tkhabisimov AB, Kachalin GV, Mednikov AF. Technological installation with high-power pulsed magnetron discharge for forming wear-resistant coatings on the surface of elements of thermal power equipment. *Natural and Technical Sciences*. 2013;1(63): 171-177. (In Russian)
30. Ryzhenkov AV, Volkov AV, Mednikov AF, Tkhabisimov AB, Zilova OS, Sidorov SV. Results of measurements of substrate deformation and determination by bending of internal stresses in Ti-TiC-DLC coating obtained by using HIPIMS technology. *Materials Physics and Mechanics*. 2021;47(2): 285–292.
31. Tretyakov RS, Krivobokov VP, Yanin SN. Technological capabilities of the magnetron diode with an evaporating target. *Izvestiya vuzov. Fizika*. 2011;54(1/3): 288–293. (In Russian)
32. Kachalin GV, Medvedev KS, Kasyanenko VA, Mednikov AF, Tkhabisimov AB. Study of the growth rate and structure of chrome coating obtained by magnetron sputtering from uncooled target. *Current Issues in Energy*. 2024;1(6): 25–29. (In Russian)